

Microyield and fracture in polycrystalline MgO

M. N. SINHA, D. J. LLOYD, K. TANGRI

Metallurgical Science Laboratory, Department of Mechanical Engineering, University of Manitoba, Winnipeg, Manitoba, Canada

Microyield and plastic flow occurring in polycrystalline MgO prior to fracture at room temperature is examined. It is shown that the initial dislocation activity occurs in the region of grain boundaries at a stress independent of grain size and below the microyield stress. The microyield stress corresponds to the stress necessary for propagating slip across the grain diameter but is below the stress necessary to produce dislocation activity in adjacent grains. The microyield stress obeys a Petch type of relationship with respect to grain size and this is attributed to the variation of dislocation density with grain size. The fracture stress - grain size relationship also follows the Petch equation but indicates that extensive work hardening has occurred prior to fracture.

1. Introduction

In recent years there have been many investigations of the strength of ceramics - see Davidge and Evans [1] for a recent review. While these materials are normally referred to as brittle, it is now generally accepted that the majority fracture with the aid of plastic flow (Petch [2]). Thus the theory due to Griffith [3], which refers to the purely elastic spreading of inherent flaws, is not strictly valid. Orowan [4] suggested that the Griffith equation be modified to

$$\sigma_F = \left(\frac{2E\gamma_t}{\pi C} \right)^{\frac{1}{2}} \quad (1)$$

where σ_F is the fracture stress; E is Young's modulus; C is the crack length; $\gamma_t = \gamma_s + \gamma_p$; γ_s is the thermodynamic surface energy per unit area of surface and γ_p is the plastic work associated with fracture.

Recently, Evans [5] has carried out a detailed investigation of the factors influencing γ_t in Equation 1, and concluded that γ_p is the major contribution to γ_t . In addition the presence of plastic flow in the fracture of alumina has been suggested by Congleton and Petch [6] and in uranium dioxide by Daniel and Takahashi [7].

The influence of plastic flow in brittle fracture is supported by the fact that the fracture stress obeys a Hall-Petch relationship with respect to grain size:

$$\sigma_F = \sigma_0 + k_F d^{-\frac{1}{2}} \quad (2)$$

where σ_F is the fracture stress, σ_0 is a frictional stress, d is the grain size and k_F is a constant.

In the case of magnesium oxide Equation 2 has been supported by the recent experiments of Evans and Davidge [8]. Carniglia [9] has considered the fracture of several other brittle materials in terms of Equation 2.

It is therefore well established that plastic flow accompanies fracture in most ceramic systems. The plastic flow involved however, is very limited and one is therefore dealing with micro-stain behaviour (in the present context micro-strain refers to strains $< 10^{-5}$). This paper reports part of a study aimed at quantitatively detecting microyield in ionic solids, together with an evaluation of the mechanisms giving rise to microyield.

2. Experimental techniques

Fully dense, 99.9% pure polycrystalline MgO was obtained from Eastman Kodak Company, USA, the major impurity being about 100 ppm Fe. The slabs were cut into flat tensile specimens of dimensions (5.0 × 0.6 × 0.1 cm), using a precision wafering machine. Each specimen was mechanically polished on a series of metallographic papers followed by diamond paste polishing and chemical polishing in hot 85% orthophosphoric acid. The chemical polishing was repeated after the final heat-treatment. The required range of grain sizes was produced by

heating at 1800 and 1650°C for various periods of time. Some of the specimens were annealed in a vacuum of 10^{-6} torr while others were annealed in air. The two different atmospheres were used since the recent experiments by Moon and Pratt [10] suggest that the form of the iron impurity has a significant influence on the mechanical properties of MgO single crystals.

The tensile tests were carried out on a tensometer attached to an X-ray diffractometer, similar to the arrangement described by Swaroop and Tangri [11]; this permits the simultaneous measurement of uniaxial tensile stress (through a calibrated stainless steel load cell), the total uniaxial strain (through a resistance strain gauge fixed to the specimen), and lattice strain (ϵ_z) in a direction perpendicular to the direction of pulling, from shifts in X-ray line peak positions. The lattice strain in the direction of straining was obtained by dividing ϵ_z by ν , the Poisson's ratio. The accuracy of the total strain measurements was $\pm 1 \times 10^{-6}$ and that of X-ray line shifts was $\pm 1 \times 10^{-5}$ Å. The high-angle reflecting planes (4 2 0) and 4 2 2), with Ni-filtered $\text{CuK}\alpha$ radiation, were used for the X-ray experiments. Further details of the X-ray experimental techniques can be obtained from Swaroop and Tangri [11].

The dislocation structure in the as-annealed condition and after deformation was examined by etch pitting in 50% (by volume) H_2SO_4 at 60°C for 1 to 2 min. All specimens were strained at a crosshead speed of about 10^{-5} min^{-1} .

3. Results

Fig. 1 is a typical plot of total strain and lattice strain against stress for two grain sizes. Up to a certain value of applied stress the lattice strain is proportional to the applied strain and this is the elastic region of the curve. Beyond this region of proportionality the lattice strain deviates from the total strain and on unloading there is a residual lattice strain (this can be seen by drawing a line parallel to the elastic line from the lattice strain curve to the strain axis). Since residual lattice strain is indicative of plastic flow (see for example the review by Greenough [12]), the stress at which lattice and total strain values deviate is considered to be the microyield point. Such curves can be represented in a more familiar form as in Fig. 2, where stress is plotted against plastic strain for three grain sizes. It should be noted however, that the plastic strain values in Fig. 2 include any strain resulting from crack formation.

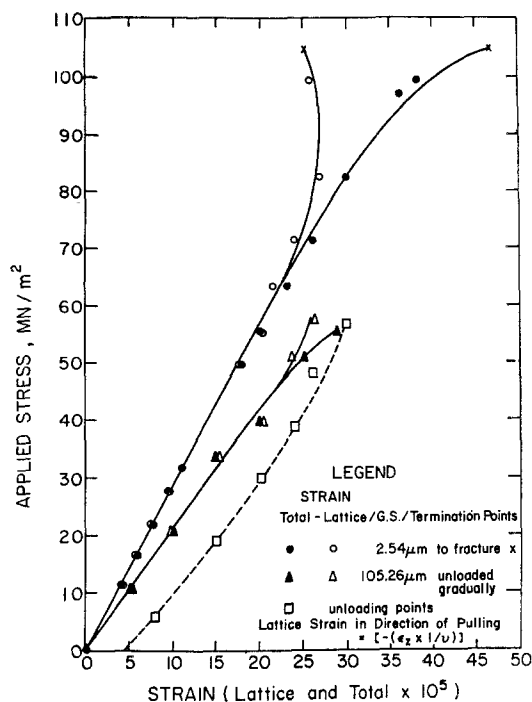


Figure 1 Applied stress against lattice and total strain.

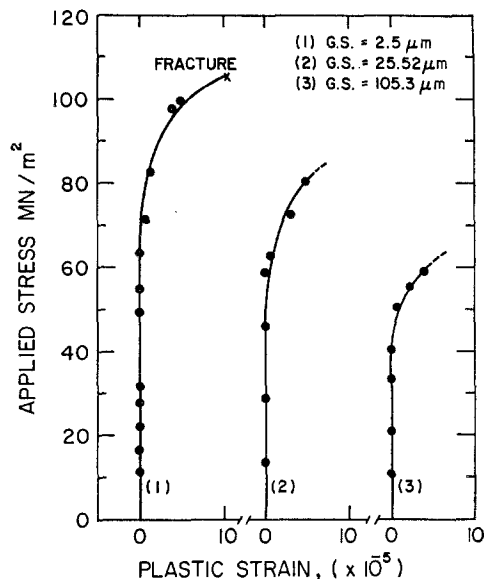


Figure 2 Stress-strain curves for different grain sizes.

Fig. 3 is a plot showing the grain size dependence of the stress at which slip activity was first detected by etch pitting, of the microyield stress, of the flow stress at 3×10^{-4} strain and of the fracture stress. It is apparent that the yield, flow and fracture stresses obey a Hall-Petch relation-

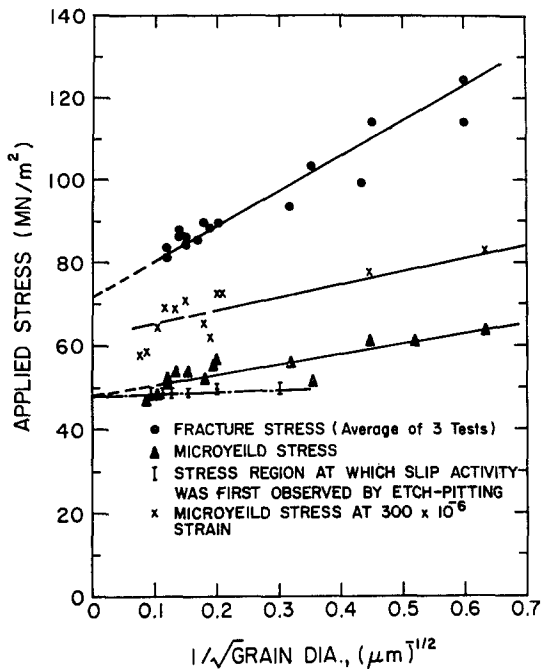


Figure 3 Stress-grain size plots for the slip initiation stress, microyield stress, microyield stress at 3×10^{-4} strain and fracture stress.

ship within experimental error. However, the intercepts and gradients of the curves differ. The stress at which slip was first detected by etch pitting is relatively independent of grain size over the range of grain sizes where reasonable reproducibility could be obtained.

3.1. Etch pit structure

The initial dislocation density (ρ) after heat-treating was obtained by etch pit measurements using the formula $\rho = (N^2M/A)$ where N is the number of pits in an area A of the micrograph, and M is the magnification. About 20 grains were measured on each specimen. Fig. 4 shows that the initial dislocation density is grain size dependent, increasing with decreasing grain size. It should be noted however, that dislocation etch pitting on MgO is to some extent, orientation dependent. Thus the absolute values of the dislocation densities in Fig. 4 are likely to be low, while the profile of the curve is not expected to be greatly in error.

Fig. 5 shows a typical example of the first evidence of slip activity, and it can be seen that this initial slip is closely associated with the grain boundaries, often occurring in regions of stress concentration such as triple points. As the stress

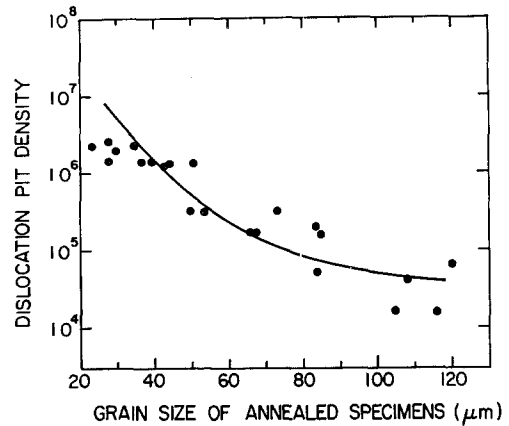


Figure 4 Graph showing the variation of initial dislocation density with grain size.

is increased the extent of slip activity also increases until at the microyield stress slip has spread across the major portion of the grain diameter (Fig. 6). With further increase in stress the slipbands broaden and gradually fill the grain interiors and also spread into adjacent grains (Fig. 7). At fracture the slip activity has spread to colonies of grains, each grain of the colony being filled with slip activity.

4. Discussion

Two points should be noted before considering the results. All the specimens were chemically polished and microscopically examined to ensure that no surface damage was present prior to testing. Thus plastic flow and cracking is not a result of surface flaws, which can have a significant effect on the deformation and fracture of MgO (Evans and Davidge [8]). Furthermore, the microyield stress is defined as the stress at which the lattice and total strains are no longer proportional. Beyond this stress residual lattice strain is present on unloading the specimen, and since residual lattice strain is clear evidence of plastic deformation (Greenough [12] and Swaroop and Tangri [11]) the microyield stress is associated with plastic flow rather than crack formation. In view of the limits of accuracy with which strain measurements were made, the microyield stress represents the flow stress for about 5×10^{-6} strain.

4.1. Slip initiation

The micrographs clearly show that the first evidence of slip is associated with grain boundaries, the majority of dislocation pile-ups

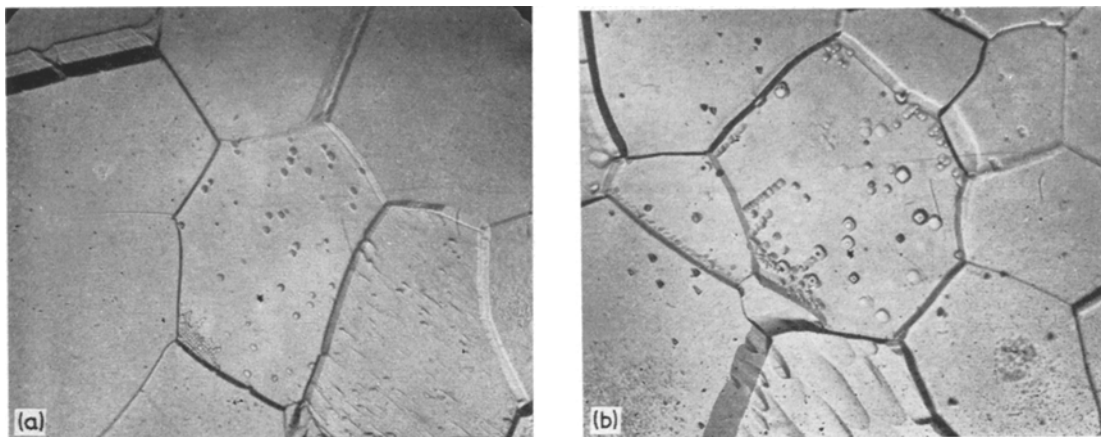


Figure 5 Examples of slip initiation from grain boundaries. (a) $\times 200$ (b) $\times 350$.

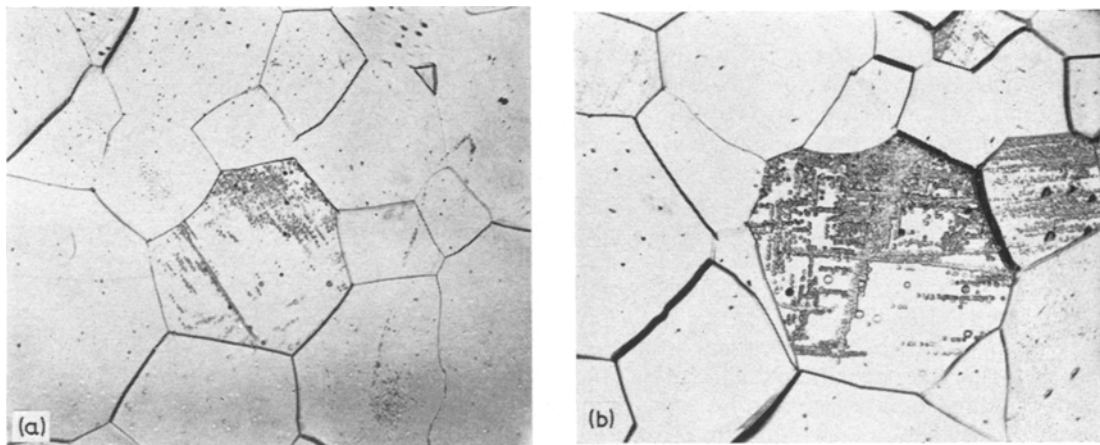


Figure 6 Representative micrograph showing the slip-bands traversing the entire grain diameter. (a) $\times 110$ (b) $\times 170$.

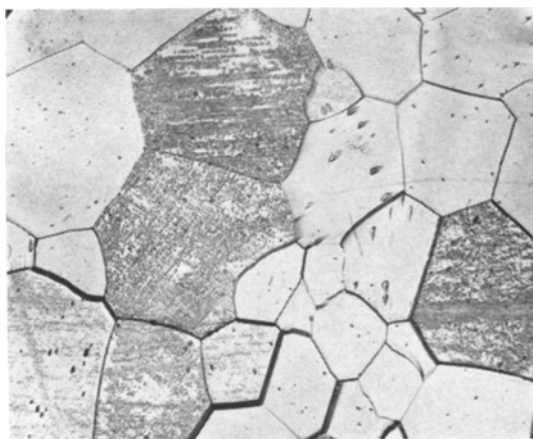


Figure 7 Micrograph showing the slip activity at stresses approximately 80% of fracture stress, $\times 110$.

formed have one end in contact with the grain boundary. The etch patterns are very similar to those found in Fe-3% Si by Worthington and Smith [13] and are probably produced by activation of grain boundary sources. Recently, Baro and Hornbogen [14] have attributed the grain size dependence of the flow stress to the operation of grain boundary sources:

$$\sigma_y = \sigma_{\text{GB}} + k_{\text{GB}} l^{-\frac{1}{2}} \quad (3)$$

where σ_{GB} is the stress opposing the motion of grain-boundary dislocations, l is the length of the grain boundary pile-up and is assumed proportional to d , the grain size, and k_{GB} is a constant involving the shear modulus of the boundary and the Burgers vector of grain-boundary dislocations.

Fig. 3 shows however, that the stress to

nucleate grain-boundary sources is relatively independent of grain sizes for grain sizes larger than 10 μm . Again, similar results were obtained on Fe-Si by Suits and Chalmers [15]. Thus the results are not in agreement with Equation 3 and the model of Baro and Hornbogen. Several models have been suggested for grain-boundary sources. Li [16] suggested that grain-boundary ledges can act as donors of dislocations. The problem with this mechanism is that ledges are not regenerative, i.e. they do not give rise to a Frank-Read source type mechanism, and cannot supply the large number of dislocations observed. Price and Hirth [17] have modified the ledge theory, suggesting that the ledge is sheared one Burgers unit along the slip plane thus nucleating a screw dislocation. Continued shearing of the ledge causes additional dislocation generation. A detailed electron microscopy investigation would be needed to determine if the Price and Hirth mechanism was viable. However, the etching characteristics of some of the initial pile-ups suggested that they were of edge character rather than screw. Finally, Baro and Hornbogen [14] have postulated that lattice dislocations can be created at the head of a grain-boundary dislocation pile-up, mainly at regions of stress concentration such as triple point junctions. The critical concept in this model is the free slip distance l , of the grain-boundary dislocations in the actual boundary. For slip in the boundary the Burgers vector of the grain-boundary dislocation and the line of the dislocation must be contained in the boundary. Thus any kink or change of direction of the boundary will limit the free slip distance over which the necessary requirements are met. In deriving Equation 3 Baro and Hornbogen assumed $l \propto d$, however, this may not be the case. Instead, l may be determined by the misorientation across the grain boundary and a simple grain-size dependence of the stress for grain-boundary source activation may not be the case.

It is apparent however, that the initial slip activity occurs from grain boundaries, with dislocation sources lying in or very close to the boundary. In addition, the sources must be regenerative since many dislocations are produced from the same region of boundary.

4.2. Microyield

The results of Fig. 3 show that the microyield stress obeys the Hall-Petch relationship with

respect to grain size. Petch [18] postulated that dislocation pile-ups form against the grain boundary resulting in a stress concentration at the head of the pile-up nucleating slip in the adjacent grain. A similar model was suggested by Cottrell [19], both associate the grain size relationship with the propagation of slip across grain boundaries. The etch pitting experiments show that, contrary to the above models the microyield stress is associated with slip band formation within the grains and examples of slip break-through of grain boundaries at the microyield stress were extremely rare. Hence, the pile-up models do not appear applicable for the microyield stress - grain size relationship.

Alternative models are the work hardening and the grain-boundary source models. The work hardening models, such as those of Conrad *et al* [20] and Ashby [21] consider the flow stress as being proportional to the square root of the dislocation density according to

$$\sigma = \sigma^* + \alpha\mu b\sqrt{\rho} \quad (4)$$

where σ is the flow stress, σ^* is the thermal component of the flow stress, ρ is the average dislocation density, μ is the shear modulus, b is the Burgers vector and α is a constant.

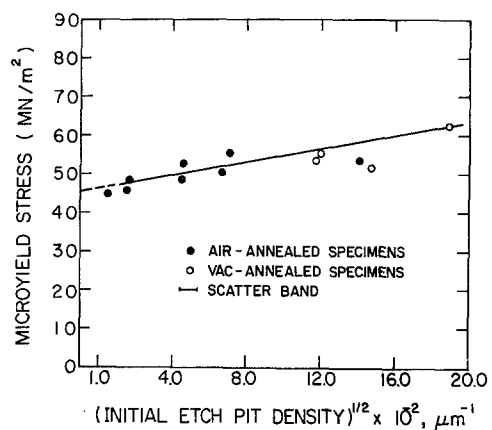


Figure 8 Variation of microyield stress with (initial dislocation density)^{1/2}.

Fig. 8 is a plot of the microyield stress against (initial dislocation density)^{1/2} and it can be seen that a straight line relationship is obtained with a gradient of $\sim 0.8 \times 10^{-4} \text{ MN m}^{-1}$, corresponding to a value of $\alpha \approx 1.5$. The work hardening models then suggest that the subsequent accumulation of dislocations with continued straining is grain size dependent with $\rho \propto 1/d$. In

detail the various models differ, for example, in the theory of Conrad *et al* the intercept of the Petch plot should be strain independent. However, Fig. 3 indicates that the intercept increases with increasing strain. On the other hand the Ashby model is in qualitative agreement with the results.

An alternative model is the grain boundary source model of Li [16] and Li and Chou [22]. They postulate that yielding is from grain-boundary ledges and assuming a constant ledge density, the number of dislocations produced is proportional to the grain-boundary surface area. Thus a Petch type relationship is again obtained. With the limited strain range available it is not possible to decide on the operative model. The results indicate however, that the work hardening and grain-boundary source models are in general agreement with the results, and that the microyield stress is controlled by the initial dislocation density.

A further point should be made regarding the microyield data of Fig. 3 and that is that the specimens heat-treated in air show identical behaviour to those annealed in vacuum, both sets of specimen lying on the same straight line. The specimens treated in air should maximize the Fe³⁺ ions while those annealed in vacuum should have mainly Fe²⁺ as impurities. Moon and Pratt [10] found that the flow stress increased with increasing ferric concentration for MgO single crystals deformed in compression. Since the Fe impurity content of the present polycrystalline MgO is 100 ppm and Moon and Pratt reported the effect in single crystals containing 10 to 150 ppm iron, sufficient iron impurity should be present to give an effect. It may be that the iron impurities are concentrated at the grain boundaries and are not as effective strengtheners in this region as they are in the lattice.

4.3. Fracture

As shown in Fig. 3 the fracture stress – grain size relationship also follows a Hall-Petch type equation

$$\sigma_F = \sigma_0 + k_F d^{-\frac{1}{2}} \quad (5)$$

where σ_F is the fracture stress; σ_0 is some frictional stress; d is the grain size and k_F is a constant, independent of grain size.

Comparison of the fracture stress – grain size plot with the microyield stress plot reveals several interesting features. The first point of interest is that the intercept σ_0 is much larger than the

intercept of the yield stress line. The much larger σ_0 in the fracture stress situation reflects the extensive work hardening that the matrix has undergone following initial yield.

In a very elegant experiment on bicrystals Ku and Johnston [23] showed that Equation 5 was valid (in their case d was the glide-band length) and suggested that σ_0 was the stress for dislocation multiplication. The present experiments show that dislocation multiplication occurs at a much lower stress, multiplication occurring in the region of the microyield stress. On the other hand, Evans and Davidge [8] have associated σ_0 with the flow stress of single crystals. The present results would indicate that microstrain should be possible in single crystals at a much lower stress, corresponding with the intercept for the microyield curve. The macroscopic yield stress in single crystals, however, may be much larger and in the region of σ_0 . The main point is that significant plastic flow and work hardening occurs in polycrystalline MgO prior to fracture. This is also evident from the etch pit experiments.

Fig. 3 also shows that the gradient k_F of the fracture stress curve is much larger than k_Y for the microyield curve. k_F is the effective shear stress necessary for crack nucleation which, according to the more recent calculations of Smith and Barnby [24] is expected to be larger than k_Y for yielding, regardless of which yielding mechanism is operating. The majority of crack nucleation occurred at grain boundaries similar to the mechanism suggested by Zener [25] and observed in bicrystals by Ku and Johnston [23]. Occasionally however, crack nucleation occurred at the intersection of two slip bands in the grain interior. Fig. 9 shows crack nucleation at the intersection of two 120° slip bands, one slip band contains about 70 dislocations while the other contains about 20. These numbers of dislocations are in the range expected for crack nucleation on the basis of calculations by Chou and Whitmore [26] for pile-ups intersecting at 120°. Chou and Whitmore assumed that a stress concentration of 10³ was required at the head of the pile-ups and calculated that about 60 dislocations are required in the pile-up. The major fracture mode, however, was cracking at grain boundaries, but the crack propagation path depended on grain size. At grain sizes smaller than 25 μm the fracture path was mainly intergranular, while for grain sizes larger than 50 μm it was transgranular with a mixed character for grain sizes 25 to 50 μm.

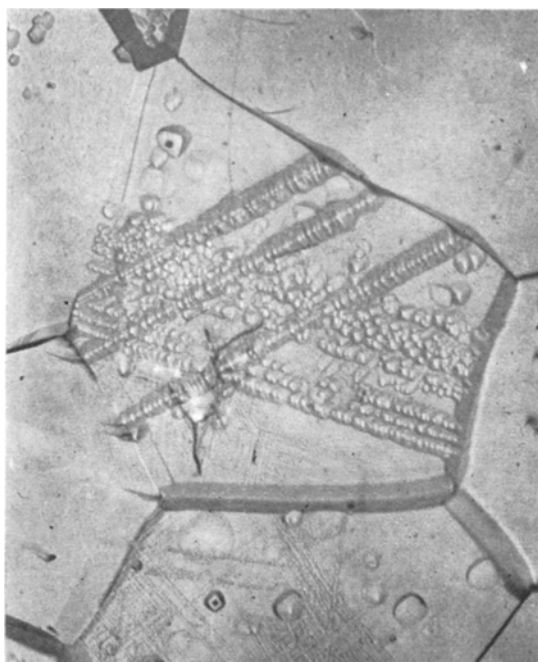


Figure 9 Microcrack nucleated at the intersection of two slipbands, $\times 300$.

5. Summary

The present experiments have clearly shown the presence of plastic flow prior to fracture in polycrystalline MgO. Dislocations are initially produced from sources in or very close to the grain boundary. The stress for activation of these sources is independent of grain size for grain sizes larger than $10\ \mu\text{m}$.

The microyield stress shows a Hall-Petch relationship in terms of grain size. Since slip breakthrough is rare at the microyield stress, the grain size dependence is attributed to the change in dislocation density with grain size. It was also found that the microyield stress appeared to be independent of ferric ion concentration, unlike the situation in single crystal MgO.

The fracture stress also obeys a Hall-Petch relationship in terms of grain size. The intercept stress, σ_0 is much larger than the equivalent stress for yield and this is attributed to the extensive work-hardening that occurs prior to fracture. The gradient of the fracture stress – grain size plot is also larger than that for yield as expected on theoretical grounds.

Acknowledgement

The authors wish to thank the Atomic Energy of Canada Limited for financial support.

References

1. R. W. DAVIDGE and A. G. EVANS, *Mat. Sci. Eng.* **6** (1970) 281.
2. N. J. PETCH, "Fracture", ed H. Liebowitz, (Academic Press, London, 1968) p. 351.
3. A. A. GRIFFITH, *Phil. Trans. Roy. Soc. London* **221A** (1920) 163.
4. E. OROWAN, "Fatigue and Fracture of Metals" (Wiley, New York, 1950) p. 139.
5. A. G. EVANS, *Phil. Mag.* **22** (1970) 841.
6. J. CONGLETON and N. J. PETCH, *Acta Metallurgica* **14** (1966) 1179.
7. J. L. DANIEL and S. TAKAHASHI, "Proc 1st International Conf. on Fracture", Sendai (eds T. Yokobori, T. Kawasaki, and J. L. Swedlow, 1965) p. 1987.
8. A. G. EVANS and R. W. DAVIDGE, *Phil. Mag.* **20** (1969) 373.
9. S. C. CARNIGLIA, *Mater. Sci. Res.* **3** (1966) 425.
10. R. L. MOON and P. L. PRATT, *Proc. Brit. Ceram. Soc.* **15** (1970) 203.
11. B. SWAROOP and K. TANGRI, *Trans. Met. Soc. AIME*, **245** (1969) 61.
12. G. B. GREENOUGH, "Progress in Metal Physics" (Pergamon Press, London, 1952) p. 190.
13. P. J. WORTHINGTON and E. SMITH, *Acta Metallurgica* **12** (1964) 1277.
14. G. BARO and E. HORNBOKEN, "Quantitative Relation Between Properties and Microstructures", eds D. G. Brandon and A. Rosen, (Israel University Press, Haifa, 1969) p. 457.
15. J. C. SUITS and B. CHALMERS, *Acta Metallurgica* **9** (1961) 854.
16. J. C. M. LI, *Trans. Met. Soc. AIME* **227** (1963) 239.
17. C. W. PRICE and J. P. HIRTH, *Mat. Sci. Eng.* **9** (1972) 15.
18. N. J. PETCH, *J. Iron Steel Inst.* **173** (1953) 25.
19. A. H. COTTRELL, *Trans. Met. Soc. AIME* **212** (1958) 192.
20. H. CONRAD, S. FERNERSTEIN, and L. RICE, *Mat. Sci. Eng.* **2** (1967) 157.
21. M. F. ASHBY, *Phil. Mag.* **21** (1970) 399.
22. J. C. M. LI and Y. T. CHOU, *Met. Trans.* **1** (1970) 1145.
23. R. C. KU and T. L. JOHNSTON, *Phil. Mag.* **9** (1964) 231.
24. E. SMITH and J. T. BARNBY, *Met. Sci. J.* **1** (1967) 56.
25. C. ZENER, "Fracturing of Metals" (American Society for Metals, 1948) p. 3.
26. Y. T. CHOU and R. W. WHITMORE, *J. Appl. Phys.* **32** (1961) 1920.

Received 2 June and accepted 26 June 1972.